Proof-Of-Concept Robot Platform for Exploring Automated Harvesting of Sugar Snap Peas

V. F. Tejada · M. F. Stoelen · K. Kusnierek · N. Heiberg · A. Korsaeth

Abstract Currently, sugar snap peas are harvested manually. In high-cost countries like Norway, such a labour-intensive practise implies particularly large costs for the farmer. Hence, automated alternatives are highly sought after. This project explored a concept for robotic autonomous identification and tracking of sugar snap pea pods. The approach was based on a combination of visible (VIS) - near infrared (NIR) reflection measurements and image analysis, along with visual servoing. A proof-of-concept harvesting platform was implemented by mounting a robotic arm with hand-mounted sensors on a mobile unit. The platform was tested under plastic greenhouse conditions on potted plants of the sugar snap pea variety *Cascadia* using LED-lights and a partial shade. The results showed that it was feasible to differentiate the pods from the surrounding foliage using the light reflection at the spectral range around 970 nm combined with elementary image segmentation and shape modelling methods. The proof-of-concept harvesting platform was tested on 48 representative agricultural environments comprising dense canopy, varying pod sizes, partial occlusions and different working distances. A set of 104 images were analysed during the teleoperation experiment. The true positive detection rate was 93% and 87% for images acquired at long distances and at close distances, respectively. The robot arm achieved a success rate of 54% for autonomous visual servoing to a pre-grasp pose around targeted pods on 22 untouched scenarios. This study shows the potential of developing a prototype robot for semi-automated sugar snap pea harvesting.

Keywords low-cost robotics, performance evaluation, semi-automated harvesting, spectral reflectance, sugar snap peas

Introduction

V. F. Tejada
Department of Systems Engineering and Automation, Universidad Carlos III de Madrid, 28911 Leganés, Madrid, Spain
Centre for Robotics and Neural Systems (CRNS), University of Plymouth, PL4 8AA Plymouth, UK
e-mail: virginia.fernandezdetejada@plymouth.ac.uk

M. F. Stoelen
Centre for Robotics and Neural Systems (CRNS), University of Plymouth, PL4 8AA Plymouth, UK

K. Kusnierek · A. Korsaeth
Department for Agricultural Technologies and System Analysis, Norwegian Institute of Bioeconomy Research (NIBIO), PO Box 115, NO-1431 Ås, Norway

N. Heiberg
Gartnerhallen SA, PO Box 111, NO-1081 Oslo, Norway

Precision Agric (2017) 18:952–972
DOI 10.1007/s11119-017-9538-1
The final publication is available at link.springer.com

The horticultural sector is characterized by a large number of manual tasks. This applies in particular to the harvest operation, where a major concern is to ensure product quality during the harvesting process in order to maximise the market value. As a consequence, the harvesting of many horticultural crops is highly labour intensive and inefficient in terms of both time and economy. At the same time, stakeholders indicate that there is a shortage of qualified and competent employees in the sector, since it does not appear to be perceived as an attractive career choice (McIntyre, 2014).

In Norway, like in several other northern European countries, the high costs of labour are significantly weakening the competitiveness of the horticultural sector, a sector which is considered to have a huge potential, not least in Europe (McIntyre, 2014). One example is the market for sugar snap peas in Norway, which is growing rapidly, but which relies mainly on imports from Kenya, Peru and Guatemala. Today, there are only six Norwegian producers of sugar snap peas for the grocery market. The import volume has increased from 63 t in year 2000 to 1305 t in 2015, whereas Norwegian production has been in the range of 40-404 t (147 t on average) over the last six years (Green producers cooperation, Norway 2016). The consumer shelf-price of packaged sugar snap peas was in 2016 around 60 NOK (6.5 EUR) per kg.

One of the largest sugar snap pea growers in Norway is located at Torbjørnrød farm, and the production here is a good illustration of the labour demand related to this production (Fig. 1). The current harvesting operations at Torbjørnrød include a staff of 60 pickers, the majority working from mid-July to mid-September. Most of the workers are foreign nationals, and the farm has sleeping quarters, a mass kitchen and large communal areas for these workers. A gross estimate of the costs related to the yearly manual harvesting on this farm is 3 million NOK (327.000 EUR).

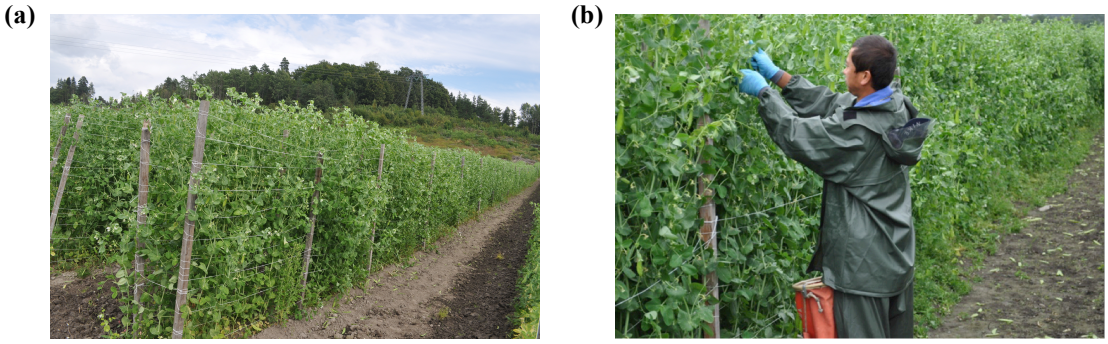

Fig. 1. Sugar snap peas of variety Cascadia at Torbjørnrød farm. (**a**) Typical field-grown environment. (**b**) A worker during the harvesting season.

The integration and development of technology in agricultural environments holds the potential to make farming operations more efficient. For high-value crops destined for fresh consumption, there are, however, few mechanized harvesting solutions on the market. For sugar snap peas, the harvesting process requires dexterity and the ability to determine quickly the correct size of the pods and, to the authors' knowledge, this crop is so far only being harvested by hand. This implies that the production is highly dependent on a large number of skilled workers. Agricultural robots can provide technological solutions to address these problems by performing selective farming tasks with autonomy, and with a *softer touch* than mechanical harvesters (Li et al. 2011). However, developing and integrating autonomous robotic systems into agricultural environments is still a challenge, due to the large variations in weather, light and terrain conditions. Moreover, automated agricultural solutions must deal with crops which may

Precision Agric (2017) 18:952–972
DOI 10.1007/s11119-017-9538-1
The final publication is available at link.springer.com

offer large variability in terms of colour, shape and size, and frequently are partially occluded by leaves (Bac et al. 2014).

Autonomous harvesting robots have been investigated and tested over recent decades to enhance the profitability and productivity of the horticultural sector. In the EU-funded CROPS project, a robot for harvesting sweet peppers in greenhouses was constructed (Hemming et al. 2014). The system was mounted on two carrier modules, one with a 9 degrees of freedom (DOF) manipulator and a second with an illumination rig. Multiple RGB and time of flight (TOF) cameras were used. Van Henten et al. (2002) presented an autonomous robot for harvesting cucumbers in the Netherlands. Their robotic system had a 7 DOF industrial manipulator mounted onto an autonomous vehicle, and two vision systems were used for detection and 3D location of the fruit. The average picking cycle rate was 45 s per cucumber, with a success rate of 80%. In New Zealand (Scarfe et al. 2009), a kiwifruit-harvesting robot was developed in the form of an autonomous mobile vehicle equipped with four custom-designed picking arms achieving, with each of the four robotic arms, a cycle time of 1 s per fruit; the fastest picking rate ever reached by a harvesting robot. Hayashi et al. (2010) designed a strawberry-harvesting robot in Japan. This was a 3 DOF manipulator with an end-effector for suction and non-suction picking operations, a machine vision system with LED illumination integrated, and a travelling platform, achieving a picking time of 11.5 s. In general, these harvesting robots have high initial investment costs and thus long payback periods. Until now, the typical robotic system for horticulture has not passed the proto-type stage and made commercially available, with some exceptions (Agrobot SL, Huelva, Spain; F. Poulsen Engineering ApS, Hvalsø, Denmark; Wall-Ye, Mâcon, France).

The overall goal of this project was to design and evaluate a proof-of-concept robot for semi-automated harvesting of sugar snap peas. An essential factor in robotic harvesting systems is the ability to accurately identify and autonomously harvest mature fruit. Therefore, this paper presents a method for autonomous identification and tracking of sugar snap pea pods on growing plants during the motion of the robot arm, as a first step towards developing a robust prototype for harvesting sugar snaps peas in open field conditions.

Materials and Methods

Spectral Reflectance Analysis of Sugar Snap Pea Plants

Colour is one of the most common visual cues employed by machine vision algorithms in harvesting robots, especially when the fruits have colour features different from the rest of the environment. Particularly, the RGB space is exploited in agricultural vision systems, e.g. for citrus fruit harvesting (Hannan et al. 2007). A recent approach on broccoli heads identification employed colour-based segmentation techniques in combination with an all-around enclosure to completely block the sunlight (Kusuman et al. 2016). However, under unstructured outdoor field conditions, colour-based segmentation is very hard to achieve due to the huge variations in outdoor illumination conditions and shadows that the robot may encounter in the field (Bulanon et al. 2002; Hannan and Burks 2004). A first approach was attempted to directly separate the pods from the leaves (Stoelen et al. 2015), by using the Hue Saturation Value (HSV) colour

Precision Agric (2017) 18:952–972
DOI 10.1007/s11119-017-9538-1
The final publication is available at link.springer.com

model to explore segmentation by colour in open field. Given the geometry of sugar pea plants, an all-around shade covering both the robot arm and the plant canopy was not feasible to use to significantly block the ambient illumination. Hence, a more robust method for a visual segmentation of the sugar snap pea pods was searched, and possible differences in the spectral signature between pods and leaves and stems (Kondo and Endo 1988) were therefore explored. To do so, measurements of sugar snap pea pods were performed using a spectroradiometer (ASD FieldSpec 3, ASD Inc., Boulder, USA), with a spectral range between 350 and 2500 nm. The reflectance spectra were obtained by calibrating the radiance reflected from the object with a white reference panel (Spectralon, Labsphere, North Sutton, USA). In order to compare the objects with different intensities, a min-max normalization was applied to the reflectance spectra. The reflectance maxima occurred at a wavelength of 850 nm and the minimum values were sampled at 400 and 670 nm for leaves and pods, respectively. The results showed clear differences in the spectral signatures of pods and leaves around 970 nm, a finding which was exploited in the proof-of-concept robot platform presented here. Spectral imaging has also been used in other studies for recognition of fruits and foliage with similar apparent colours, in fruits such as cucumbers (Kondo et al. 1996; Van Henten et al. 2002; Noble and Li 2012), green citrus (Lee 2007; Okamoto and Lee 2009, 2010) and grapes (Kondo et al. 1996).

Proof-Of-Concept Harvesting Robot

The overall idea in this project is that a fleet of semi-autonomous robot systems, supervised by human operators, should be available when needed by the farmer. In this way, the number of robotic platforms can be adapted to the size of the harvesting job, even for smaller farms. The study presented here aimed at developing a proof-of-concept harvesting robot, maintaining a simple robotic technology. This was considered to be crucial for keeping the unit cost low, and thereby reducing the need for farmers to commit to investments in large and expensive hardware up front. An early proof-of-concept harvesting robot was therefore designed and implemented for testing the identification and tracking of sugar pea pods, keeping the previous requirements in mind. The overall design consisted of a 4-wheel drive base that formed the mobile platform for the robotic manipulator, and a robot arm placed on the top of a static mount for testing purposes (Fig. 2). The cutting device was not investigated in this early prototype. The aim here was instead to be able to place the end-effector in the correct position for the cutting action, i.e. by positioning the fingers of the gripper around the stem of the sugar pea pod. Initial tests showed that a partial shade combined with an active light source had to be integrated in order to maintain similar illumination conditions under highly variable ambient lighting conditions, as encountered both in a field and in a greenhouse.

Robot Arm

For the robot manipulator arm, a small 5 DOF robot from Trossen Robotics (Downers Grove, USA) was selected, the WidowX Mark II. This low-cost and lightweight (1.5 kg) robot arm is based on the Dynamixel daisy-chained servos, providing high-accuracy ($\geq 0.088^{\circ}$) and flexible control through adjustable Proportional Integral Derivative (PID) parameters. The onboard microcontroller (ArbotiX Robocontroller, Vanadium Labs

Precision Agric (2017) 18:952–972
DOI 10.1007/s11119-017-9538-1
The final publication is available at link.springer.com

LLC., NY, USA) is operated through the Robot Operating System (ROS) stack available, which greatly simplifies the integration of the whole system. The robot has a vertical working range of 410 mm, while carrying a maximum payload of 300 g at half-extended configuration. The overall weight of the vision system equipment was 250 g including the supporting structure.

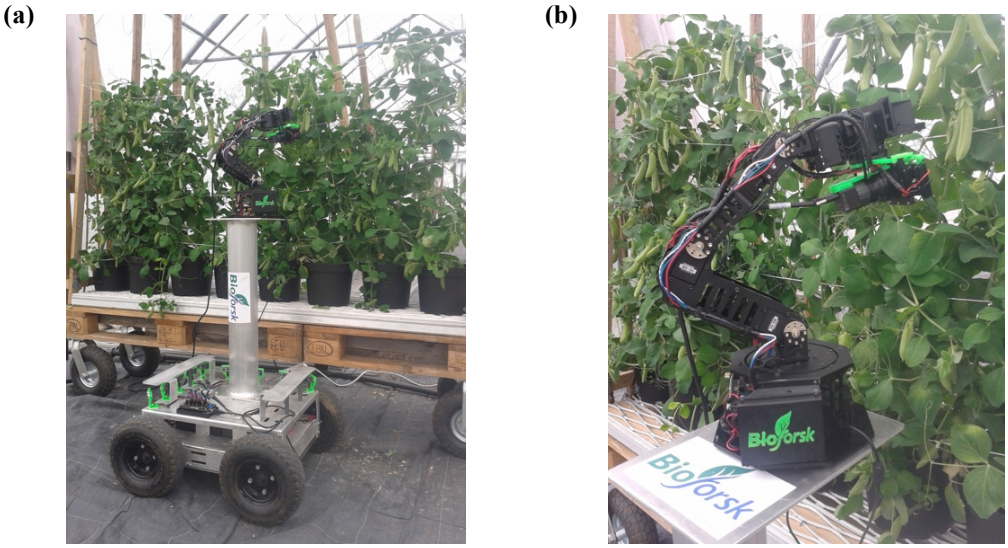

Fig. 2 Proof-of-concept of sugar snap pea harvesting robot facing sugar pea plants. (**a**) View of the complete system: mobile platform, static mount and robot arm. (**b**) Close-up view of the robotic arm without a partial cover. See Figure 5b for the partial cover used during the experiments.

For the current proof-of-concept, it was decided to attempt to pre-grasp the sugar snap pea pods during the picking process. Thus, an infrared proximity breakout sensor (Vishay VCNL4000, SparkFun Electronics, Niwot, USA) was attached below the fingers of the 1DOF parallel gripper to measure the distance from the cutting point to the nearest part detected of the targeted pod within a range of 20-50 mm. This infrared sensor has a detection region that can be modelled as a cone-shaped zone with an effective angle of ±20º, and a peak intensity wavelength centred at around 890 nm.

Vision System

A grey-scale, USB3 vision CCD camera with enhanced sensitivity in the NIR (MQ013RG-E2, Ximea GmbH., Münster, Germany) was mounted below the robot wrist enabling an optimal perspective of the sugar snap pea pods in the scene. This lightweight camera (27 g) enabled the carrying capabilities of the robot arm and provided high-resolution images (up to 1.3 megapixel) at a maximum frequency of 60 frames per second, which was sufficient to maintain real-time performance.

The camera was equipped with a lens (Theia SY110M, Theia Technologies LLC., Wilsonville, USA) allowing objects in the scene like pods, stems and leaves to remain in sharp focus without any lens adjustment, while the robot approached to the targeted pods from a distance of about 100-120 mm. The selected lens also offered a wide field of view without distortion (up to 130º diagonally), thus covering large regions of interest. Its infrared (IR) corrected optics for use with LED illumination up to 950 nm ensured high transmission of the NIR light around 940 nm. A long-pass filter (Knight Optical Ltd., Harrietsham, UK) was attached to the front part of the lens. This filter,

Precision Agric (2017) 18:952–972
DOI 10.1007/s11119-017-9538-1
The final publication is available at link.springer.com

with a cut-on wavelength placed at 715 nm, removes the radiation in the ultraviolet and visible parts of the spectrum, transmitting the IR radiation only. The filter enabled the targeted wavebands centred at 850 nm and 940 nm to fall into the maximum transmission region. This region ensured that approximately 90% of the NIR light incident was transmitted to the imaging sensor.

To illuminate the scenes, four narrow-band IR LED modules (Intelligent LED Solutions Ltd., Berkshire, UK) were placed in pairs on each side of the optical filter. Each pair consisted of one LED module with a centroid wavelength at 850 nm (ILH-IO01-85SL-SC201-WIR200) and one with a centroid wavelength at 940 nm (ILH-IO01-94SL-SC201-WIR200). Both types of LEDs provide a radiance angle of ±45º, and about 1 W of optical power at the operating current of 1 A.

In order to minimize the effect of changing ambient light conditions, a partial shade of cardboard was used during the experiments to cover the robot arm and its workspace (Fig. 5b). Thus, the plant canopy remained out of the limits of the shade. An equivalent shade would be required for a working in-field prototype. A similar technique has also been employed with success for robotic apple harvesting (Baeten et al. 2008).

Mobile Platform

As a mobile base for the robot, a custom-designed platform (Superdroid Inc., Fuquay-Varina, USA) was used. The weight of the aluminium mobile platform was approximately 30 kg, including four 24V DC motors and two 12V-18Ah sealed lead-acid batteries. The maximum allowed payload was about 30 kg, and it could reach a maximum forward speed of 6 km/h (with the selected transmission). The mobile base was driven by all four motors, with two left and two right motors coupled together in pairs. Turning occurred by differential steering, i.e. by giving different speed to the left and right motor pairs.

Sugar Snap Pea Pod Identification and Tracking

The automated harvesting process should be designed to handle open field conditions. In the field, the light conditions are highly varying, and the pods may be moving slightly when exposed to wind. Additionally, the effect of uneven soils in outdoor agricultural scenarios commonly generate vibrations in the robotic system, making quite difficult to achieve accurate grasping in the order of millimetres over the life-time of the robot without recalibrating sensors periodically. To address these challenges, a visual servoing method was therefore explored by employing an imaging sensor mounted below the robot end-effector. Such a method implies that the pixel position in the output image can directly be related to Cartesian movements of the gripper, and thereby updating the target location while the robot arm approaches the fruit. This approach has been also applied for robotic orange harvesting (Mehta and Burks 2014) and sweet-pepper harvesting (Barth et al. 2016). An architecture for visual servoing based on the open source robot middleware ROS (version Indigo, C++ and Python) and the image processing library OpenCV (version 2.4.9, Python) running on Linux UBUNTU (version 14.04) was utilized here. The visual servoing ROS nodes were operated through the ArbotiX micro-controller ROS stack, with active light control and a custom inverse kinematics module (Fig. 3).

Precision Agric (2017) 18:952–972
DOI 10.1007/s11119-017-9538-1
The final publication is available at link.springer.com

The methodology employed for identifying sugar snap pea pods was mainly based on elementary segmentation methods such as global thresholding, as well as edge detection algorithms and shape modelling (Fig. 4). The identification of the pods was achieved by illuminating the scene with alternating LED light with 850 nm and 940 nm in consecutive cycles of 150 ms, and acquiring one image for each separate light period. The frames grabbed using the filtered imaging camera were then combined to construct an index image, by dividing the image taken at 940 nm by the image taken at 850 nm, pixel by pixel.

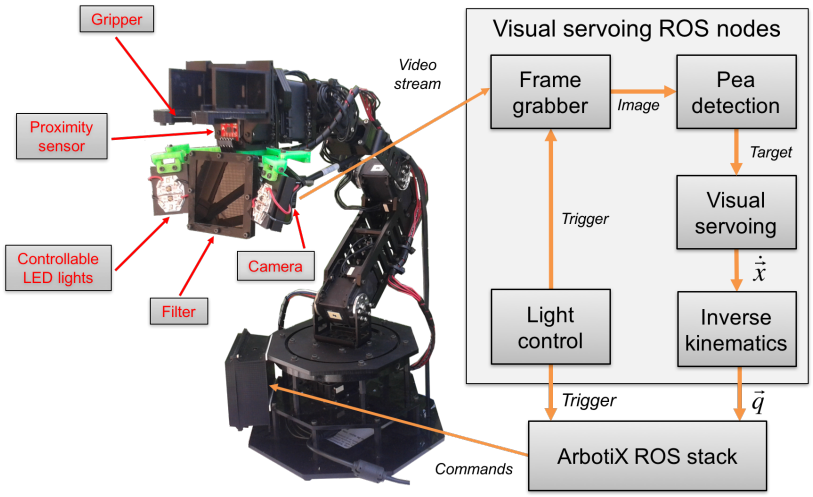

Fig. 3 Overview of the architecture used for the visual servoing of the robot arm. $\dot{\vec{x}}$ is the Cartesian velocities of the hand, $\vec{q}$ the joint angles

Given the index image, a clear separation between pods and the other parts of the plant was possible, but this required an optimal threshold value. The LED lighting system caused local illumination differences in the targeted scene when the robot was commanded towards the target. Therefore, the key concept in the segmentation approach considered here was to maintain a similar brightness (level of grey) over the robot trajectory in the acquired index images. For this purpose, a simple proportional controller was implemented to modify the exposure setting on the fly, using the brightest spot of the 850 nm image as reference. Since the exposure setting was automatically adjusted over time, an empirically determined global threshold value was predefined (100) for all the experiments.

The result obtained by the reflection-based method was further refined by analysing the texture in the images using fast algorithms for edge detection, available in OpenCV (Bradski and Kaehler 2008). One of the main features of the sugar pea pods is their relatively smooth texture compared with the leaves of the plant. This characteristic seems especially true in the horizontal direction, normal to gravity, and may thus be used as an additional filter, by removing regions with large amounts of horizontal lines (vertical gradients). For the edge detection, a Sobel algorithm was used, blending vertical and horizontal directions with equal weights (0.5). It is important to note that the parameters required for this algorithm can be difficult to determine so they were selected to be suitable for a range of different local illumination situations (depending on the active light configuration).

Considering the shape of the sugar snap pea pods, their image projection in 2D could be reasonably well modelled as elongated ellipses in the vertical direction. Such ellipses were then modelled by fitting them to the contour of the blobs obtained in the previous

Precision Agric (2017) 18:952–972
DOI 10.1007/s11119-017-9538-1
The final publication is available at link.springer.com

imaging processing step. To distinguish whether an ellipse could be considered suitable to represent a sugar snap pea pod, multiple geometrical parameters had to be satisfied for positive identification (empirically determined parameter values in parenthesis): a) the minimum and the maximum aspect ratio of the major and minor axes of the ellipse (0.05 and 0.5, respectively), b) the minimum overlapping area of the contoured region and the ellipse area (0.60), c) the maximum angle of the major axis with the vertical (65º), and d) the minimum area of the ellipse (800 pixels).

After the ellipse discrimination steps, the tracking process required that only a suitable ellipse within the field of view of the camera was selected. If several suitable ellipses were detected, the largest ellipse was selected as target. The robot arm approached the targeted ellipse making the difference in pixels between the actual position of the centre of the ellipse in each frame and the selected aim position in the image. In the case where no suitable ellipse was detected, the robot would stop performing visual servoing until an appropriate ellipse was detected in the scene. In the final step, the infrared proximity sensor measured the distance from the end-effector to the targeted ellipse. The tracking process stopped when the difference between the cutting point of the end-effector and the selected pod was lower than a predefined threshold (3mm).

Precision Agric (2017) 18:952–972
DOI 10.1007/s11119-017-9538-1
The final publication is available at link.springer.com

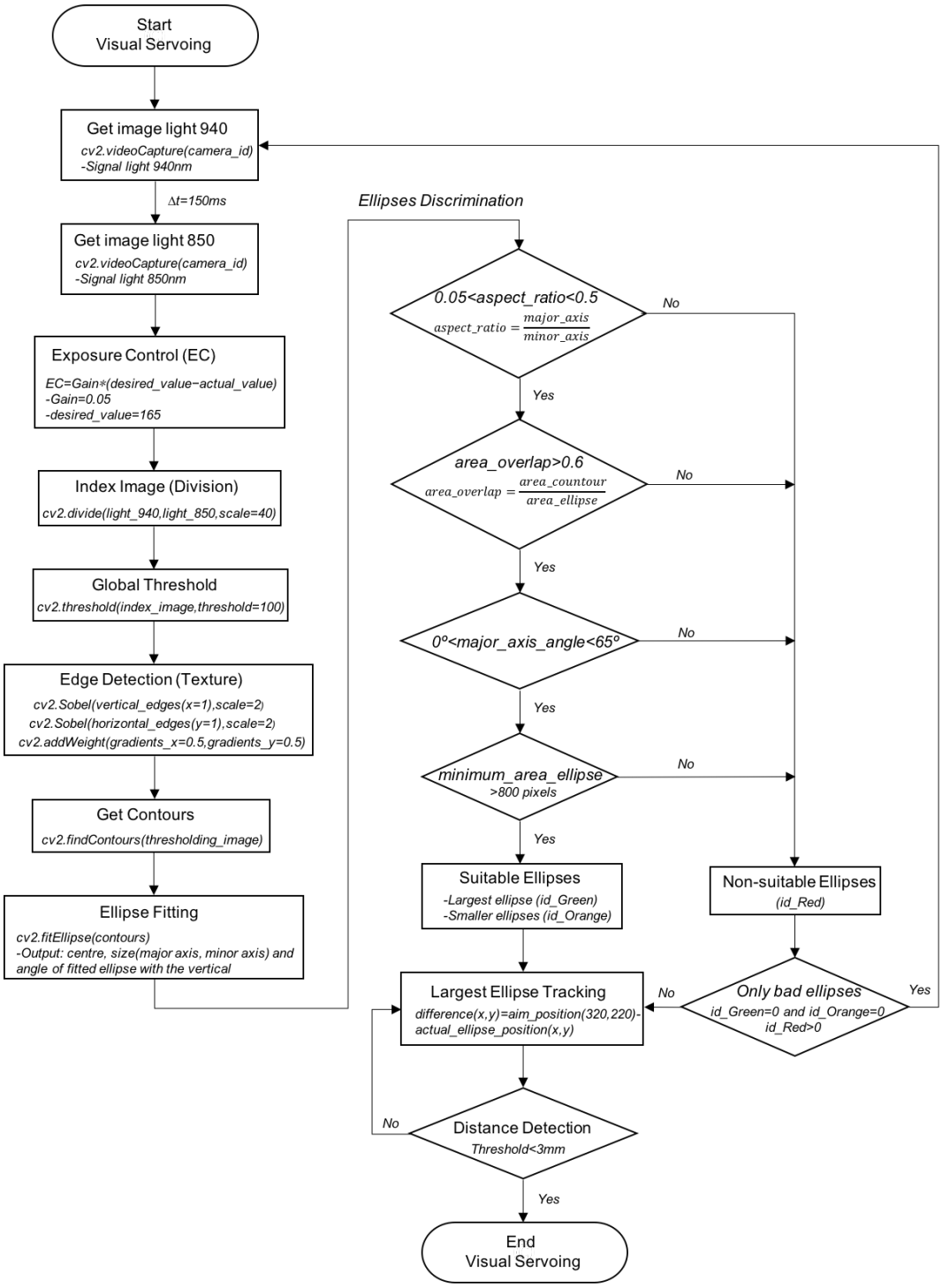

Fig. 4 Flowchart of the methodology employed for identifying sugar snap pea pods. The main OpenCV functions (cv2 prefix) are included. All parameter values were empirically adjusted.

Testing and Evaluation

Testing the actual proof-of-concept on sugar snap pea plants took place over a period of several weeks, in the spring of 2015 at NIBIO Apelsvoll research station, located in SE Norway. Test plants were produced by putting 2 seeds of variety *Cascadia* into pots, being about 210 mm in diameter, and containing 5 l of fertilized soil. The pots were also

Precision Agric (2017) 18:952–972
DOI 10.1007/s11119-017-9538-1
The final publication is available at link.springer.com

fertilized and watered regularly according to demand, and the plants were tied up in supporting strings when they reached a height of about 150 mm. About 10 pots were planted each week from beginning of March onwards, to ensure the presence of plants in the right development stage for testing.

The robotic system was tested under plastic greenhouse conditions to reduce the exposure of sugar snap pea plants to low temperatures that might adversely affect their normal growth and development. Testing conditions involved wide variations in outdoor illumination, from sunny to overcast, which heavily influenced indoor illumination. While performing the tests, the minimum temperature recorded in the greenhouse was 8.5ºC and the maximum temperature reached 34.5ºC. The relative humidity ranged from 24.5% to 80.5%.

Experimental Setup

A modular carrier was constructed to mimic a row of sugar snap pea plants as normally found in the field. The sugar snap pea testbed included a movable bench mounted on the carrier with a triangular housing attached that could be effectively adapted for eight pots (Fig. 5a). This testbed allowed both pods hanging individually or in clusters, and leaves and stems merging together to produce the typical fruit distribution, dense foliage and occlusions encountered in real growing environments.

Fig. 5 Experimental setup at NIBIO Apelsvoll. (**a**) Sugar snap pea modular carrier inside the plastic greenhouse. (**b**). Moving desk carrying the partial shade and equipment (laptop, spacenavigator and power supply). The partial shade is covering the robot arm and its working environment

While the carrier was used to facilitate the transportation of the pots in the greenhouse, a moving desk was employed to drive the robot arm with its shade and the necessary equipment (laptop, joystick and power supply) along a row of test plants to perform the experiments. Considering these practical reasons, the 4-wheel platform was not included as part of the experimental setup. The input device used for manual control of the robot was a SpaceNavigator 6 DOF joystick (3Dconnexion GmbH., Munich, Germany).

Teleoperation Experiment

Precision Agric (2017) 18:952–972
DOI 10.1007/s11119-017-9538-1
The final publication is available at link.springer.com

A first experiment was performed to quantify the detection rate of the pod identification method proposed (true positive, false positive and false negative rate summarized in Table 1), while simulating sugar snap pea pod picking tasks under teleoperation. The experimental procedure consisted of manually moving the robot arm using the SpaceNavigator joystick from an initial resting position in front of the plant canopy to the grasping position of the selected pod. The simulated picking tasks were performed on 26 untouched agricultural scenarios comprising 104 pod discrimination images. The testing scenarios were distributed over the sugar snap pea testbed, involving configurations of pods, leaves and stems that typically occur in field-grown environments such as clusters and partial occlusions. Four pod discrimination images (640x480) were acquired at different working distances per each scenario (see Trajectory range in Table 1) for post-processing analysis. The working distances were manually measured from the selected pod location in the canopy while the robot arm was tele-operated towards the targeted pods.

Visual Servoing Experiment

A second experiment was conducted to evaluate the performance of the visual servoing architecture described in Figure 4. The visual servoing approach implied that the location of the centre of a tracked pod in the visual field of the camera was used to autonomously command the robot arm towards the pod position. The relative position of the robot arm with respect to the targeted pod was measured using the proximity sensor attached to gripper. The simplified picking tasks performed consisted of automatically moving the end-effector of the robot from an initial resting position, located at the maximum detection distance measured from the pod's location on the plant canopy (see MDD metrics in Table 2), to a pre-grasping position with the fingers around the stem of a targeted pod. The overall execution cycle of the visual servoing algorithm presented in Figure 4 was running at approx. 5 Hz. VGA resolution images (640x480) were taken at each frame rate during the trajectory performed by the robot arm. The testing environment involved 22 untouched agricultural scenarios distributed over the sugar pea testbed, with varying pod sizes and surrounding foliage normally encountered in real growing scenarios. An attempt was judged as successful when the fingers of the gripper were positioned around the stem of a targeted sugar pea pod within a range of 20% of the total length of the pod, measured from the junction of the peduncle and the pod. In addition, the cycle time chosen to consider a trial successfully accomplished could not exceed 15 s. This choice was based on the low sample rate of the execution cycle selected for performing these trials.

Results

Spectral Reflectance Analysis of Sugar Snap Pea Plants

Comparing the reflectance spectra of pods and leaves, the most significant differences in the reflectance spectra were found centred at around 970 nm (Fig. 6). This waveband is correlated with water content of the target. Since pods contain more water than leaves and stems, an empirically determined threshold value could be used to discriminate the pods from the other plant parts.

Precision Agric (2017) 18:952–972
DOI 10.1007/s11119-017-9538-1
The final publication is available at link.springer.com

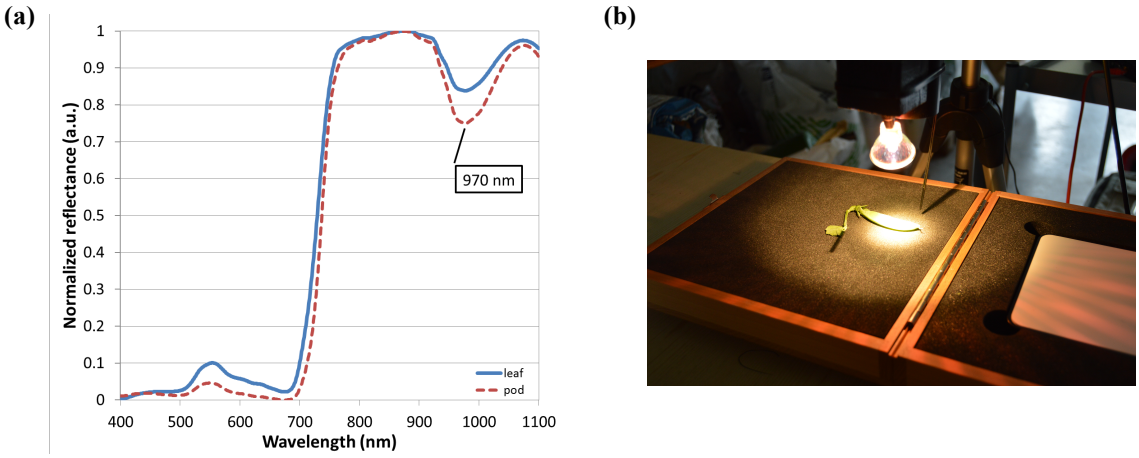

Fig. 6. Spectral reflectance analysis of sugar peas. (**a**) Normalized spectral reflectance of a pod (dashed line) and a leaf (solid line). The largest difference occurs in the 970 nm water absorption feature. (**b**) Experimental setup involving a spectro-radiometer point, a white reference panel and a sugar pea pod.

Effects of Global Threshold and Exposure Settings

The influence of the highly variable ambient illumination in the greenhouse was successfully mitigated by introducing a partial shade to cover the working environment of the robot arm during both experiments. However, setting a predefined global threshold value to separate pods from leaves typically failed in most preliminary testing scenarios (Fig. 7).

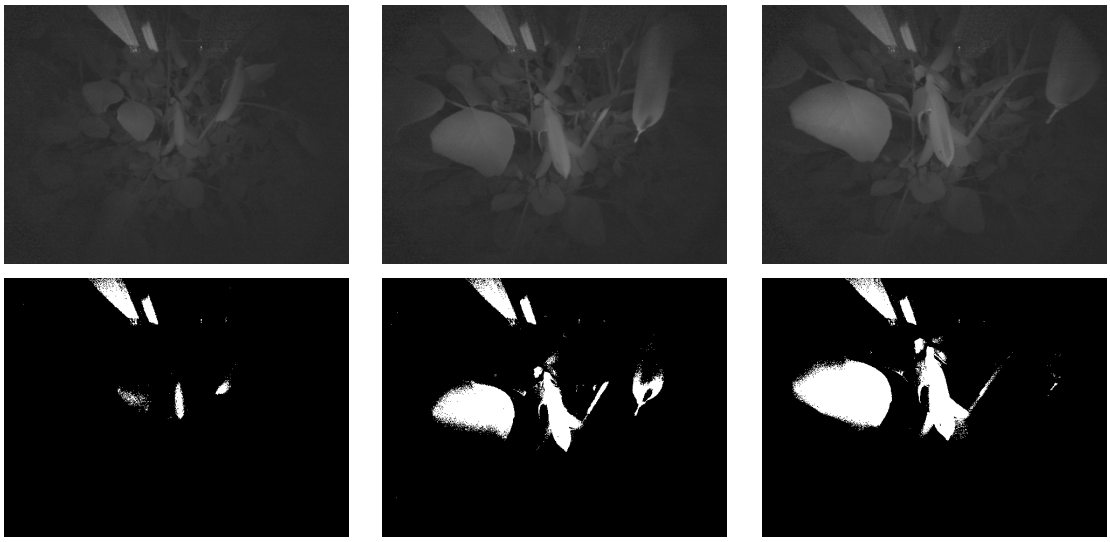

Fig. 7 Example of output images taken at different distances where pods are unsuccessfully discriminated from leaves and stems. Global threshold value was predefined (80) and the exposure setting was fixed (55) while the robot was approaching the targeted pod. (**a**) Index image (upper) and thresholding image (bottom) at 90 mm, (**b**) index image (upper) and thresholding image (bottom) at 45 mm and (**c**) index image (upper) and thresholding image (bottom) at 30 mm

This was particularly due to the influence of the LED lighting intensity on pods and leaves inside the partial shade. That is, the closer the robot was to the plant canopy, the more illuminated the detected pods and leaves around them were, providing over-

Precision Agric (2017) 18:952–972
DOI 10.1007/s11119-017-9538-1
The final publication is available at link.springer.com

exposed output images. Hence, a global threshold value set by default in combination with fixed exposure times caused poor discrimination between pods and other plant parts at close ranges. Overcoming this critical factor was essential to assure a successful harvesting operation.

This promoted the use of a more appropriate approach that automatically adjusted the exposure setting to handle local illumination variations inside the partial shade. As can be observed in Figure 8, modifying exposure times in real-time offered slight variations of the intensity of the greyscale index images taken at different distances. Therefore, employing a predefined global threshold was feasible now. Note that, in this case, only pods were highlighted from the background, whereas leaves and stems remained undetected over the whole trajectory of the robotic arm.

(a) **(b)** **(c)**

Fig. 8 Example of output images taken at different distances with automatic exposure control. A global threshold value was set by default (100). The exposure setting was automatically adjusted when the robot approached to targeted pods. (**a**) Index image with exposure setting of 55.6 (upper) and thresholding image (bottom) at 50 mm. (**b**) Index image with exposure setting of 39.5 (upper) and thresholding image (bottom) at 30 mm. (**c**) Index image with exposure setting of 25.2 (upper), and thresholding image (bottom) at nearby cutting point.

Edge Detection and Ellipse Modelling

The smooth texture of the pods, in comparison to the leaves, was exploited to further improve the pod detection. This was done through the use of an edge detection algorithm. Individual sugar pea pods could quite robustly be identified by fitting ellipses to the contours retrieved after applying a threshold on the index image, removing areas with a large amount of texture, and filtering based on geometrical characteristics following the steps described in Figure 4. Figure 9 provides various examples of sugar snap pea pod identification for different testing scenarios. If an ellipse was discriminated as suitable for the tracking process, it was represented in green in the output image, otherwise in red. When more than one suitable ellipse existed in the scene, the largest ellipse appeared in green, while the remaining ellipses representing potential targets were shown in orange.

Precision Agric (2017) 18:952–972
DOI 10.1007/s11119-017-9538-1
The final publication is available at link.springer.com

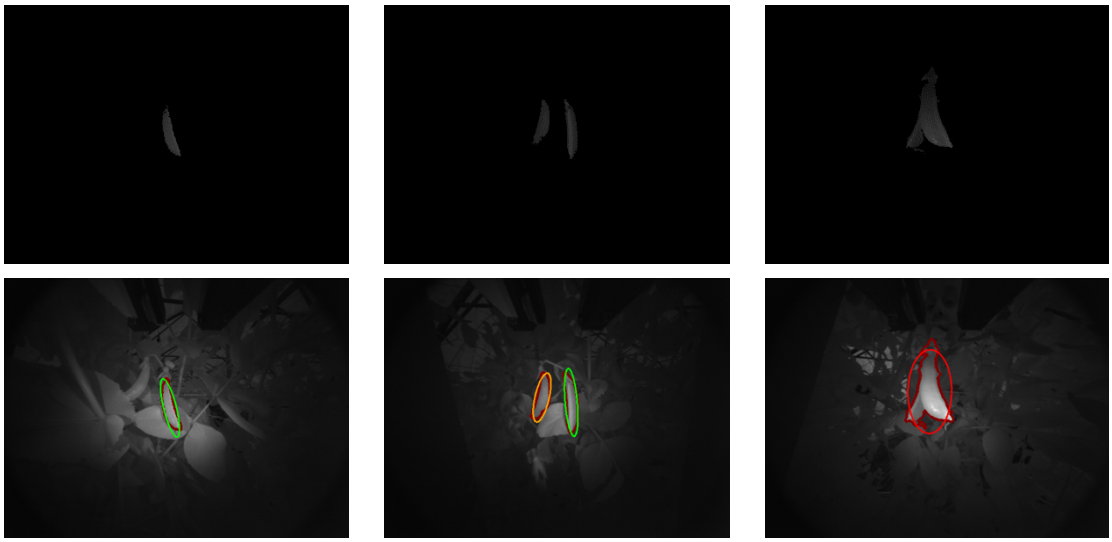

(a) **(b)** **(c)**

Fig. 9 Pod identification stage. Ellipses were fitted to contours (dark red line) and filtered based on multiple parameters: aspect ratio, minimum overlapping area, maximum orientation angle and minimum area. (**a**) *Suitable ellipse*: edge detection image (upper) and pod discriminated in green (bottom). (**b**) *Suitable ellipses*: edge detection image (upper) and pods discriminated in green (larger) and orange (smaller). (**c**) *No suitable ellipse*: edge detection image (upper) and overall shape of a cluster discriminated in red due to overlapping area criteria mismatched (bottom)

Performance Evaluation during Teleoperation Experiment

The results of the teleoperation experiment showed the potential for using the approach proposed to successfully identify sugar snap pea pods from the background. Figure 10 shows two typical scenes at different distances involving sugar snap pea plants, where pods are hanging vertically in a cluster and surrounded by leaves and stems.

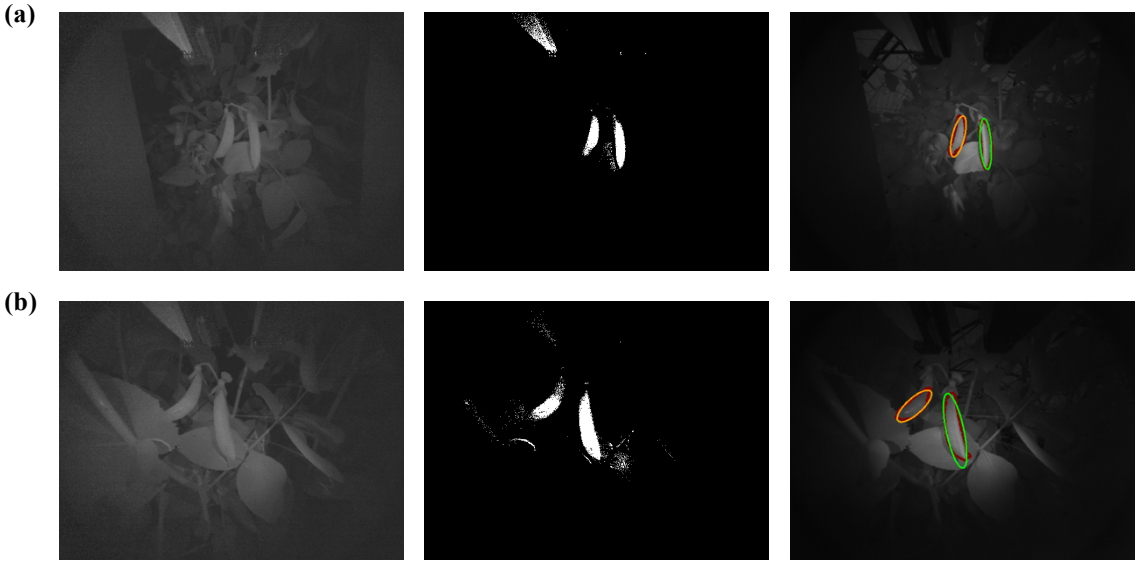

Fig. 10 Example of images taken from 2 testing scenes (true positive). (**a**) First scenario at 70 mm: index image with exposure setting of 85.9 (left), thresholding image (centre) and pod detection image (right). (**b**) Second scenario at 50 mm: index image with exposure setting of 39.3 (left), thresholding image (centre) and pod detection image (right)

Precision Agric (2017) 18:952–972
DOI 10.1007/s11119-017-9538-1
The final publication is available at link.springer.com

Since the influence of ambient illumination was effectively controlled with a partial cover, predefined values were empirically determined and applied to all the testing scenes. Moreover, the adjustment of the exposure setting in real-time meant that index images taken from different scenarios at different distances had similar brightness (Figs. 10a and 10b, left plots). Hence, a predefined global threshold was used to successfully distinguish pods from their surrounding foliage independently of the working distance (Figs. 10a and 10b, centre plots). The shape of the pods was then modelled as elongated ellipses and correctly classified into suitable fruits by the discrimination method, where larger pods were identified in green, while smaller ones were represented in orange (Figs. 10a and 10b, right plots).

However, some limitations were encountered while conducting these trials. One major drawback of the robot design was related to the LED illumination rig. The lighting system could easily be occluded by the outer leaves of the plants, providing over-exposed areas in the output images where leaves happened to block the LED sources (Fig. 11a). When this occurred, the global thresholding step could not discriminate over-exposed leaves (and/or stems) from pods (Fig. 11a, centre plot).

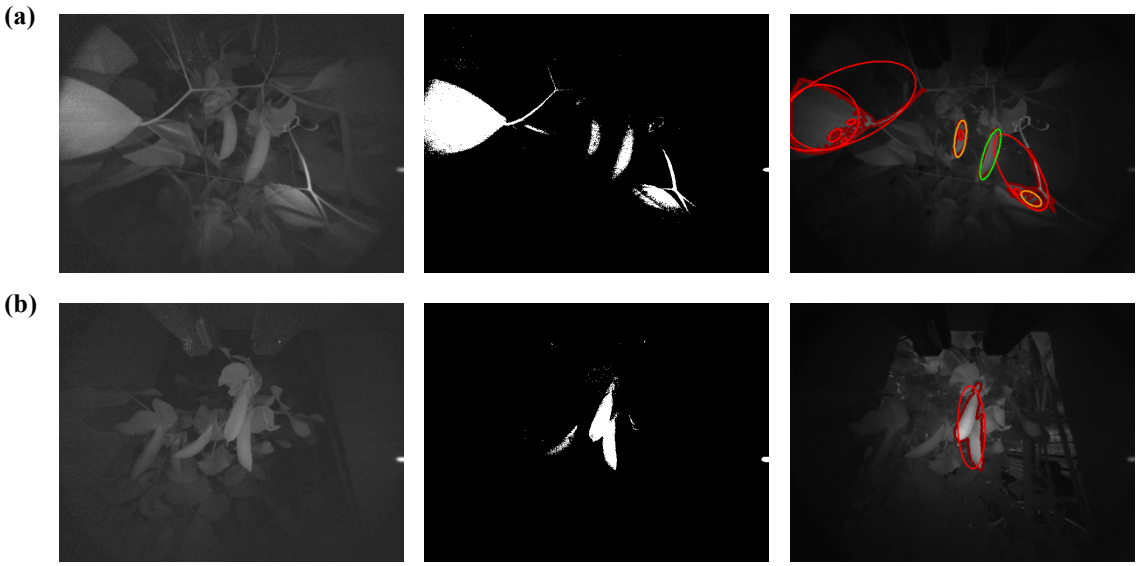

Fig. 11 Sample images of limited performance encountered in testing scenarios. (**a**) Occlusion by leaves at 30 mm: index image (left), thresholding image (centre) and pod detection image (right). (**b**) Overlapping criteria mismatched (false negative) at 25 mm: index image (left), thresholding image (centre) and pod detection image (right)

Nevertheless, the ellipses discrimination steps based on geometrical characteristics (see Fig. 4) typically identified and modelled the shape of the surrounding leaves and stems as no suitable ellipses in red, consequently rejecting them from the further tracking process (Fig. 11a, right plot). Another important shortcoming regarding the methodology employed for the pod identification can be observed in Figure 11b. In this example, the ellipses discrimination steps in the algorithm were not capable of discriminating each individual pod when they appear close together in a cluster, i.e. with overlay. That is, only the overall shape of the cluster could be retrieved and thus the overlapping area criterion on the region of the pods and the fitted ellipse was not satisfied (Fig. 11b centre and right plots). This implies that multiple pods close together

Precision Agric (2017) 18:952–972
DOI 10.1007/s11119-017-9538-1
The final publication is available at link.springer.com

in a cluster are susceptible to be classified as not suitable for the picking process (false negative) with the current method (see Overlapping clusters metrics in Table 1).

The performance evaluation of the teleoperation experiment on a total of 104 acquired images is summarized in Table 1. To assess the contribution of the working distance while the robot was approaching to the targeted pods, the dataset images were divided into 2 different trajectory ranges comprising 52 images for each distance range. Long-range images correspond with measures taken between 80 mm and 45 mm, and close-range images include results obtained between 45 mm and 10 mm, measured from the pod location. The total number of pods detected for each trajectory range is presented. True positive represent the number of pods successfully discriminated (Fig. 9) while false negative indicates the quantity of suitable pods for picking misclassified, involving single pods and overlapped pods in clusters (Fig. 10b). False positives implied false detections of pods when certain areas of the foliage were recognised as suitable ellipses.

Table 1 Metrics for performance evaluation during teleoperation experiment

Trajectory range	Pods detected	True positive	False negative		False positive
			Individual pods	Overlapping clusters	
80-45 mm	137	128	5	4	4
Proportion (%)	100%	93%	4%	3%	3%
45-10 mm	164	143	6	15	7
Proportion (%)	100%	87%	4%	9%	4%

The true positive rate was 93% over the total number of pods detected within the long-distance range whereas, for close-range distances, the methodology proposed achieved a success rate of 87%. To ensure that the LED lighting rig was not completely occluded by the outer leaves of the canopy, the closest images were taken at a minimum distance of 10 mm measured from the position of the selected pod in the canopy.

Performance Evaluation during Visual Servoing Experiment

The results of the performance evaluation of the visual servoing experiment can be seen in Table 2. An attempt to pre-grasp a targeted pod from an initial robot pose was made for each agricultural scenario. Length represents the dimension of the targeted pod along the vertical direction whereas Cutting Range (CR) represents the 20% of the total length of the targeted pod, measured from the junction of the peduncle and the pod. To consider an attempt successful, the fingers of the gripper should be positioned around the stem of the targeted pod within this range. Additionally, the execution time was limited to 15s to judge an attempt as successfully accomplished. Maximum Detection Distance (MDD) indicates the maximum detection distance of the targeted pod measured from its location on the plant canopy. This metric also corresponds with the initial resting position of the robot arm for each trial.

Precision Agric (2017) 18:952–972
DOI 10.1007/s11119-017-9538-1
The final publication is available at link.springer.com

Table 2 Metrics for performance evaluation of visual servoing trials (lengths in mm, and time in s). CR - Cutting Range (20% of Length), MDD - Maximum Detection Distance

Scenario	Length	CR	MDD	Execution time	Attempt
1	80.3	16.0	50	4.8	success
2	77.2	14.4	50	>15	fail (false negative)
3	64.1	12.8	70	8.3	success
4	55.6	11.1	50	9.1	success
5	66.1	13.2	60	>15	success
6	76.2	15.2	65	10.6	success
7	77.3	15.5	50	7.4	success
8	82.8	16.6	60	>15	fail (blocked illumination system)
9	75.1	15.0	60	>15	fail (blocked illumination system)
10	56.2	11.2	30	2.9	success
11	70.4	14.1	75	7.8	success
12	62.6	12.5	65	>15	fail (blocked illumination system)
13	62.4	12.5	65	>15	fail (blocked illumination system)
14	65.0	13.0	60	>15	fail (blocked illumination system)
15	68.2	13.6	50	3.6	success
16	55.5	11.1	55	10.5	success
17	62.3	12.5	65	6.6	success
18	57.5	11.5	60	>15	fail (blocked illumination system)
19	66.3	13.3	60	14.9	success
20	81.3	16.3	40	>15	fail (false negative)
21	62.3	12.4	70	8.3	success
22	70.0	13.4	50	>15	fail (blocked illumination system)

The success rate of pre-grasping was 54%, as 12 out of 22 trials were successfully accomplished (Table 2). Of the 10 unsuccessful approaches, the illumination system was totally blocked by the outer leaves of the plant canopy in 8 of them. In the remaining 2 cases, multiple pods occurred in a cluster, leading to mismatched overlapping areas (false negative). For all failed attempts, the tracking process stopped before reaching the targeted pod, exceeding thereby the execution time limit. No false positives were detected during these trials.

Precision Agric (2017) 18:952–972
DOI 10.1007/s11119-017-9538-1
The final publication is available at link.springer.com

Discussion

Sugar Pea Pod Identification

In this study, colour segmentation analysis could not be utilized as a reliable discriminatory factor, since sugar pea pods, leaves and stems did not show any practically useful chromatic differences. Thus, the presence of the water absorption band at 970 nm in green fruits was investigated here. The results revealed that the infrared spectral reflectance constitutes an alternative and robust method to improve the identification of sugar pea pods to an acceptable level. The teleoperation experiment showed that the true positive detection rate of sugar snap pea pods was 93% for images acquired at long distances and 87% for images taken at close distances.

A predefined global threshold on an infrared index image for segmentation of the spectral reflectance data was chosen for the experiments. Using global thresholding is a common approach for segmentation of visual cues, such as spectral reflectance (Okamoto and Lee, 2009) and colour (Tanigaki et al. 2008; Bulanon et al. 2009; Li et al. 2010). It has been stated that predefined global thresholding is likely to fail in most scenarios (Nalwa 1993). In the methodology proposed, however, the use of adjusted exposure times, combined with a predefined global threshold value, could be employed to effectively mitigate the changing local lighting conditions inside the partial shade. Moreover, the methodology tested here based on the spectral response is very sensitive to ambient illumination conditions (Yuan et al. 2010). Considering the variable lighting conditions normally encountered in the plastic greenhouse, it should be noted that the success of this approach strongly relied on the use of a partial shade to cover the operating environment of the robotic system during the experiments.

Complementary to the spectrally based segmentation, texture appearance (i.e. edge detection) was utilized to improve the separation between pods and surrounding leaves. An observation made on many horticultural crops was thereby utilized. That is, on the smooth skin of the fruit few edges can be detected, whereas high edge density represents the leaf area (Zhao et al. 2005; Okamoto and Lee 2010; Rakun et al. 2011). Given the 2D projection of sugar pea pods, modelling the shape as elongated ellipses seemed to be an appropriate choice to represent the targets in a robust way. Approaches using shape properties are increasingly utilized in robotic horticultural operations (Jimenez et al. 2000; Hayashi et al. 2002; Ling et al. 2004; Kong et al. 2010).

A major constraint of the current method was its limited ability to handle situations when pods are represented with overlapped features in 2D images such as clusters. Furthermore, the closer the gripper was to the clusters, the lower the performance was due to the increased size of the overall fitted ellipse that led to overlapping criteria mismatching (false negatives, see Table 1). A typical situation encountered in a sugar snap pea field is fruits with ill-defined positions, free form canopies and non-rigid plant structures that can accurately be approximated by simple geometrical models. In particular, sugar snap pea pods are widely distributed over the plant canopy causing overlapping leaves, stems and pods. Such partial occlusions typically encountered in this crop are challenging to predict given the stochastic nature of the agricultural setting. To address this problem, recent approaches have focused on 3D analysis of shape involving depth data to obtain optimal discrimination and location of fruits when an overlapping situation occurs. Thanh Nguyen et al. (2016) investigated the potential of combining colour imaging (RGB) and dimensional shape information (3D) using a

Precision Agric (2017) 18:952–972
DOI 10.1007/s11119-017-9538-1
The final publication is available at link.springer.com

RGB-D camera for accurate detection of apples on trees, whereas Barnea et al. (2016) provided a shape-based detection of significantly occluded fruits in 3D space regardless of their colour.

Robot Design and Sensing

The robotic system developed enabled a first proof-of-concept, as intended, but the testing also highlighted factors which need to be addressed to achieve an improved overall performance. One of the main limitations when conducting the experiments was the limited reachability of the robotic arm, along with the short and broad fingers of its gripper. The picking range covered only a small area of the sugar snap pea plants, so that many pods were beyond the reach of the gripper. Hence, there is likely a need to extend the size of the manipulator arm, and to integrate the arm with a lift mechanism to handle the full range of the bushes. A custom-designed gripper more suitable for grasping task should also be developed in conjunction with the pod identification and tracking processes.

A first implementation of the visual servoing architecture was employed for tracking harvest-ready sugar snap pea pods, using the results obtained during the discrimination process. Additionally, the robotic system will need to be completed by including a 3D imaging sensor (e.g. TOF cameras) mounted on the base of the robot platform to automatically drive the guidance of the manipulator to the initial position for the visual servoing. In Kazmi et al. (2014), the suitability of using TOF cameras for depth imaging under different illumination conditions was analysed. One way forward could consist of implementing motion planning tasks to ensure a collision-free path to rapidly approach the gripper at regions of interest where there is a high probability of target pods, and to safely transfer and release the picked sugar pea snap pods into a collection mechanism.

The findings revealed that the active illumination system implemented represented a major limitation while conducting teleoperation and visual servoing tracking trials. Both the number of pods detected and the overall performance of the tracking process were adversely affected by inhomogeneous illumination of the lighting system, as seen in Table 2. Also, the LED lighting system was insufficient to mitigate the ambient illumination coming from the other side of the plant, which was not covered by the partial shade, especially under sunlight conditions. Thus, considerable variations in the cycle time and MDD metrics throughout the testing scenarios can be observed in Table 2. This also explained the decreased number of pods detected for long-range distances as shown in Table 1. Moreover, the adjustment of the parameter values in the algorithm was influenced by the illumination variations presented in the testing scenarios. Therefore, a high brightness LED lighting system that provides 360º uniformity and larger coverage in the field of view of the camera is required. It should be pointed out that both the robot arm and the visual servoing algorithm can be run at a much higher frequency rate than what was used here (5 Hz), likely leading to shorter execution times. This can be achieved through, for example, optimized C code, replacing the prototype Python code used here, and by taking advantage of Graphical Processor Units (GPU).

Conclusions

Precision Agric (2017) 18:952–972
DOI 10.1007/s11119-017-9538-1
The final publication is available at link.springer.com

A proof-of-concept harvesting platform was developed to evaluate the performance of autonomous identification and tracking of sugar snap pea pods under representative agricultural environments. The combination of VIS-NIR reflection analysis, global thresholding, image-based texture analysis and shape modelling appears to be a suitable method for discriminating between sugar snap pea pods and the surrounding foliage, such as leaves and stems. This method, however, relies on a partial shade and an active light source system that minimize the effect of changes in ambient light conditions. In the current study, a global threshold combined with exposure times adjusted in real-time were used to successfully distinguish pods from leaves independently of the working distance of the robotic arm. Additionally, shape modelling analysis revealed that fitting ellipses to pod contours using geometrical parameters can be effectively applied for pod identification in different plant canopy scenarios. However, discrimination of individual pods using this approach was limited by the presence of partial occlusions in such agricultural scenes. Given the dense foliage environment, a more robust image processing method that incorporates spatial location is crucial for optimal pod identification and location. A set of 104 images were analysed during teleoperation experiments achieving a true positive rate of 93% and 87% for long distance images (80-45 mm) and close distance images (45-10 mm), respectively. The success rate of the visual servoing trials on 22 untouched environments was 54%. Findings from the teleoperation and visual servo control experiments represent an opportunity to improve the pod detection and tracking methodology and the LED illumination system to enhance the automated harvesting operation. The overall performance achieved in this study showed promising results in developing a harvesting prototype for field-grown conditions.

Acknowledgements The authors would like to acknowledge Unni Myrheim Roos and Torkel Gaardløs at NIBIO Apelsvoll, for their skilled and helpful technical assistance during the development and testing process of this study. Also thanks to Morten F. Johansen at Torbjørnrød farm for providing feedback during the design process.

References

Bac, C. W., Henten, E. J., Hemming, J., & Edan, Y. (2014). Harvesting Robots for High-value Crops: State-of-the-art Review and Challenges Ahead. *Journal of Field Robotics*, *31*(6), 888-911.

Baeten, J., Donné, K., Boedrij, S., Beckers, W., & Claesen, E. (2008). Autonomous fruit picking machine: A robotic apple harvester. In *Field and Service Robotics* (pp. 531-539). Berlin Heidelberg, Germany: Springer.

Barnea, E., Mairon, R., & Ben-Shahar, O. (2016). Colour-agnostic shape-based 3D fruit detection for crop harvesting robots. Biosystems Engineering, 146, 57-70.

Barth, R., Hemming, J., & van Henten, E. J. (2016). Design of an eye-in-hand sensing and servo control framework for harvesting robotics in dense vegetation. Biosystems Engineering, 146, 71-84.

Bradski, G., & Kaehler, A. (2008). *Learning OpenCV: Computer vision with the OpenCV library*.., Sebastopol, USA: O'Reilly Media, Inc.

Precision Agric (2017) 18:952–972
DOI 10.1007/s11119-017-9538-1
The final publication is available at link.springer.com

Bulanon, D. M., Kataoka, T., Ota, Y., & Hiroma, T. (2002). AE—automation and emerging technologies: a segmentation algorithm for the automatic recognition of Fuji apples at harvest. *Biosystems Engineering*, *83*(4), 405-412.

Bulanon, D. M., Burks, T. F., & Alchanatis, V. (2009). Image fusion of visible and thermal images for fruit detection. *Biosystems Engineering*, *103*(1), 12-22.

Green producers cooperation, Norway (2016). http://www.grontprodusentene.no/prisinformasjon-alle-kulturer. (in Norwegian) Last accessed 22 March 2017

Hannan, M. W., & Burks, T. F. (2004). Current developments in automated citrus harvesting. Paper No. 043087, ASABE, St Joseph, MI, USA

Hannan, M. W., Burks, T. F., & Bulanon, D. M. (2007). A real-time machine vision algorithm for robotic citrus harvesting. Paper No. 073125, ASABE, St Joseph, MI, USA

Hayashi, S., Ganno, K., Ishii, Y., & Tanaka, I. (2002). Robotic harvesting system for eggplants. *Japan Agricultural Research Quarterly: JARQ*, *36*(3), 163-168.

Hayashi, S., Shigematsu, K., Yamamoto, S., Kobayashi, K., Kohno, Y., Kamata, J., et al. (2010). Evaluation of a strawberry-harvesting robot in a field test. *Biosystems Engineering*, *105*(2), 160-171.

Hemming, J., Bac, C., van Tuijl, B., Barth, R., Bontsema, J., Pekkeriet, E. et al. (2014), A robot for harvesting sweet-pepper in greenhouses. *In Proceedings of the International Conference of Agricultural Engineering*. EurAgEng, Cranfield, UK, (pp. 1-8).

Jimenez, A. R., Ceres, R., & Pons, J. L. (2000). A survey of computer vision methods for locating fruit on trees. *Transactions of the ASAE*, *43*(6), 1911-1920.

Kazmi, W., Foix, S., Alenyà, G., & Andersen, H. J. (2014). Indoor and outdoor depth imaging of leaves with time-of-flight and stereo vision sensors: Analysis and comparison. *ISPRS Journal of Photogrammetry and Remote Sensing*, *88*, 128-146.

Kondo, N., & Endo, S. (1988). Calculation of the most suitable wavelength bands for discrimination between fruit and leaves using their spectral reflectance. *Scientific Reports of the Faculty of Agriculture-Okayama University (Japan)*.

Kondo, N., Monta, M., & Fujiura, T. (1996). Fruit harvesting robots in Japan. *Advances in Space Research*, *18*(1), 181-184.

Kong, D. Y., Zhao, D. A., Zhang, Y., Wang, J. J., & Zhang, H. X. (2010). Research of apple harvesting robot based on least square support vector machine. In *International Conference on Electrical and Control Engineering ICECE,* (pp. 1590-1593). Wuhan, China: IEEE.

Kusumam, K., Krajník, T., Pearson, S., Cielniak, G., & Duckett, T. (2016). Can you pick a broccoli? 3D-vision based detection and localisation of broccoli heads in the field. In *IEEE/RSJ International Conference on Intelligent Robots and Systems, IROS* (pp. 646-651). Daejeon, Korea: IEEE.

Lee, W. S. (2007). Multispectral imaging for in-field green citrus identification. Paper No. 073025, ASABE, St Joseph, MI, USA.

Li, B., Wang, M., & Wang, N. (2010). Development of a real-time fruit recognition system for pineapple harvesting robots. Paper No. 1009510, ASABE, St Joseph, MI, USA.

Li, P., Lee, S. H., & Hsu, H. Y. (2011). Review on fruit harvesting method for potential use of automatic fruit harvesting systems. *Procedia Engineering*, *23*, 351-366.

Precision Agric (2017) 18:952–972
DOI 10.1007/s11119-017-9538-1
The final publication is available at link.springer.com

Ling, P., Ehsani, R., Ting, K. C., Chi, Y. T., Ramalingam, N., Klingman, M. H., et al. (2004). Sensing and end-effector for a robotic tomato harvester. *Paper* No. 043088, ASABE, St Joseph, MI, USA.

McIntyre, A. (2014). Report on the future of Europe's horticulture sector – strategies for growth. *Report A7-0048/2014 of the Committee on Agriculture and Rural Development*, European Parliament (pp. 17). http://www.europarl.europa.eu/sides/getDoc.do?pubRef=-//EP//TEXT+REPORT+A7-2014-0048+0+DOC+XML+V0//EN Last accessed 22 March 2017

Mehta, S. S., & Burks, T. F. (2014). Vision-based control of robotic manipulator for citrus harvesting. *Computers and Electronics in Agriculture*, *102*, 146-158.

Nalwa, V. S. (1993). *A guided tour of computer vision* (Vol. 1). Reading, MA, USA: Addison-Wesley.

Noble, S. D., & Li, D. (2012). Segmentation of greenhouse cucumber plants in multi-spectral imagery. In *International Conference of Agricultural Engineering.* EurAgEng, Cranfield, UK, (pp. 1-6).

Okamoto, H., & Lee, W. S. (2009). Green citrus detection using hyperspectral imaging. *Computers and Electronics in Agriculture*, *66*(2), 201-208.

Okamoto, H., & Lee, W. S. (2010). Machine vision for green citrus detection in tree images. *Environmental Control in Biology*, *48*(2), 93-99.

Rakun, J., Stajnko, D., & Zazula, D. (2011). Detecting fruits in natural scenes by using spatial-frequency based texture analysis and multiview geometry. *Computers and Electronics in Agriculture*, *76*(1), 80-88.

Scarfe, A. J., Flemmer, R. C., Bakker, H. H., & Flemmer, C. L. (2009). Development of an autonomous kiwifruit picking robot. In *4th International Conference on Autonomous Robots and Agents, ICARA* (pp. 380-384). Wellington, New Zealand: IEEE.

Stoelen, M. F., Kusnierek, K., Tejada, V. F., Heiberg, N., Balaguer, C., & Korsaeth, A. (2015). Low-Cost Robotics for Horticulture: A Case Study on Automated Sugar Pea Harvesting. In (Stafford, J V, Ed.) Proceedings of the *10th European Conference on Precision Agriculture*, Wageningen Academic Publishers, The Netherlands, pp. 283-290.

Tanigaki, K., Fujiura, T., Akase, A., & Imagawa, J. (2008). Cherry-harvesting robot. *Computers and Electronics in Agriculture*, *63*(1), 65-72.

Thanh Nguyen, T., Vandevoorde, K., Wouters, N., Kayacan, E., De Baerdemaeker, J. G., & Saeys, W. (2016). Detection of red and bicoloured apples on tree with an RGB-D camera. Biosystems Engineering, 146, 33-44.

Van Henten, E. J., Hemming, J., Van Tuijl, B. A. J., Kornet, J. G., Meuleman, J., Bontsema, J., et al. (2002). An autonomous robot for harvesting cucumbers in greenhouses. *Autonomous Robots*, *13*(3), 241-258.

Yuan, T., Li, W., Feng, Q., & Zhang, J. (2010). Spectral Imaging for Greenhouse Cucumber Fruit Detection Based on Binocular Stereovision. Paper No. 1009345, ASABE, St Joseph, MI, USA.

Zhao, J., Tow, J., & Katupitiya, J. (2005). On-tree fruit recognition using texture properties and color data. In *IEEE/RSJ International Conference on Intelligent Robots and Systems, IROS* (pp. 263-268). Edmonton, Canada: IEEE.

Precision Agric (2017) 18:952–972
DOI 10.1007/s11119-017-9538-1
The final publication is available at link.springer.com